Full Paper

Corrosion Protection of Carbon Steel by Highly Processable Conducting Polyaniline doped Phosphoric Acid and Dodecyl benzenesulfonic Acid

Ahmad Rouhollahi* and Mohammad Hamed Barzegar Khaleghi

Department of Chemistry, K. N. Toosi University of Technology, Tehran, Iran

*Corresponding Author, Tel.: +98 21 23064222; Fax: +98 21 88035187

E-Mail: Rouhollahi@kntu.ac.ir

Abstract- A processable polyaniline (PANI) was prepared via reversed microemulsion polymerization using both phosphoric acid(PA)and dodecylbenzenesulfonic acid (DBSA) as dopants. By attaching this anionic surfactant to PANI chains, solubility and hence processability of PANI in organic solvents was highly increased. Hydrophobic PANI-PA-DBSA also demonstrated better corrosion protection efficiency in comparison to the PANI synthesized without surface active agents. Polymerization of PANI-PA-DBSA was achieved via chemical oxidation of anilinemonomers inside micelles in the presence of ammonium persulfate (APS), phosphoric acidand dodecylbenzenesulfonic acid at room temperature within one hour. PANI-PA-DBSA was characterized using FT-IR, UV-Vis and XRD techniques before being used in a protective coating composed of xylene, as solvent, and epoxy resin, as matrix. The coating was applied, using dip coating method, on carbon steel specimens. Corrosion protection performance of different coatings was investigated by electrochemical impedance spectroscopy (EIS) and DC polarization techniques. According to DC polarization tests, corrosion potential of carbon steel was shifted about 0.2 V toward more noble potentials in case of optimized PANI-PA-DBSA. EIS data also illustrated a relatively smooth surface with very high resistance which couldserve as a good protective coating due to barrier effects of epoxy resin, reversible redox properties of PANI, and hydrophobicity of PANI-PA-DBSA. Moreover, for different samples, open circuit potential (OCP) was monitored versus time; based on the monitoring results, PANI-PA-DBSA with optimized DBSA content showed relatively little changes over time, as compared to other coatings. Further, different samples had their morphologies investigated using scanning electron microscopy (SEM).

Keywords- Polyaniline, Phosphoric acid, Dodecylbenzenesulfonic acid, Emulsion synthesis, corrosion protection, carbon steel

1. INTRODUCTION

In 1862, the very first report on polyaniline was published by H. Letheby [1].In 1985, Deberry [2] found that; electrically deposited polyaniline can protect steel against corrosion. Since then, organic coatings are used for corrosion protection of different metals [3]. Early conventional corrosion protection methods were using conversion steps such as phosphatation or chromatation. Despite their relatively good corrosion protection performance, their application was highly restricted by environmental protection protocols [4]. Since the discovery of polyaniline conductive nature, it has been extensively studied and used in many applications including electromagnetic shielding devises, light weight batteries and anticorrosion coatings [5]. Either as film-formingcorrosion inhibitor or protective coating, polyaniline has attracted much attention due to excellent anticorrosion ability, environmental-friendly characteristics and simple doping/dedoping chemistry [6].

Most of early reports on PANI were concentrated on electropolymerization of aniline on either stainless steel [7] or iron [8]. However, in order to produce large quantities of PANI, electropolymerization may not provide a valid option. This is when chemical oxidation reaction comes into play [9]. This process involves oxidation of aniline monomers by an oxidizing agent in the presence of suitable dopants. Both oxidizing agent and dopants are responsible for physical and chemical characteristics of the produced PANI. The choice of suitable oxidizer can vary from ammonium persulfate [10], potassium dichromate [11] and hydrogen peroxide [12] to $AgNO_3$ [13] and $CuCl_2$ [14]. Suitable doping agents can be chosen from a wide range of compounds including strong inorganic acids [15] to weak organic acids [16]. Different dopants will results in polymers with different characteristics. These characteristics may be controlled by the choice of dopant [17]. It is also possible to achieve PANI without adding any dopant through interfacial polymerization [18] or by simply dedoping PANI using NH_4OH solution [19].

PANI can act as both corrosion inhibitor and protective coating. It can serve as inhibitor due to the presence of C=N groups which can be adsorbed on the metallic substrate surface and restrain cathodic or anodic reaction [20]. PANI can be used as an anticorrosion material in both emeraldine base (EB) and emeraldine salt (ES) forms. The EB form of PANI is not conductive in nature, but it can transform into its ES form during protonation reaction in acidic environments. Corrosion protective characteristic of EB is mainly stemmed from its barrier effects, and the protection is considered to be inactive [21]. In contrary to EB, the ES form of PANI contains dopants which can be released during redox reaction on metallic surfaces. These dopants can then participate in forming a second barrier layer through reacting with metallic ions, preventing corrosion even further [22]. Several researches has been done trying to evaluate corrosion protective characteristic of PANI doped with different dopants; some of the researches have proposed that, phosphate ions represent one of the best dopants when it comes to corrosion protection using PANI [23-26]. Da Silva *et al.* proved

that, barrier effects of PANI can prevent corrosion through a two-step mechanism:1) a redox reaction between iron and PANIforms a passive layer, and 2) a second layer is formed by complex salt layer with iron and dopant ion [27]. Sathiyanarayanan *et al.* demonstrated that, incorporating PANI into an epoxy coating will increase production rate of insulate iron oxide layer at pine holes and defects via a reversible redox reaction between ES and leucoemeraldine salt (LS) of PANI [28].

Despite good overall characteristics, there are drawbacks that can seriously limit application of PANI on an industrial scale. Bulk polymerization of PANI usually results in a product which is insoluble in common organic solvents, limiting its application due to its poor processability. As revealed in literature, properties of PANI are highly dependent on its synthesis procedure and substrates [29,30]. In order to improve processability of PANI and largely enhance its potential applications, researchers have used copolymers, self-doped PANI, polymer blends, PANI dispersion using stabilizers, and PANI nanostructures [31]. In 1993, Cao *et al.* proposed emulsion polymerization route to produce processable conductive PANI [32]. Since then, different surface active agents have been used as protic acids or secondary dopants. These surfactants can lower surface tension of PANI chains, making them soluble in organic solvents [33].

According to previous researches [34-37], microemulsion systems (W/O or O/W) are valid options to prepare highly-processable PANI. The main characteristic of such a system is its ability to solubilize both hydrophilic and hydrophobic materials [38]. The most important advantage of microemulsion polymerization of aniline monomers is the opposed to other methods [39].
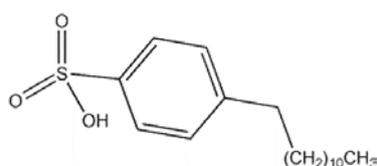
Scheme 1. DBSA structure

In this work, PANI was prepared using PA and DBSA (Scheme. 1) as protic acid and secondary dopant, respectively (PANI-PA-DBSA), in presence of APS, so as to simultaneously maximize corrosion protection performance and processability of the synthesized PANI. The synthesized PANI was used for corrosion protection of carbon steel in an epoxy resin matrix. Corrosion protection performance and characteristics of PANI-PA-DBSA were then investigated.

2. EXPERIMENTAL

2.1. Materials

Aniline (An) (99%), DBSA (97%) and phosphoric acid (85%) were purchased from Sigma Aldrich (USA). Ammonium persulphate (98%) was purchased from Panreac (Spain). Chloroform, Epoxy resin (EP-400) and epoxy hardener (Ep-100-86) were purchased from local manufacturers (Amertat Co. and Pars Pamchal Chemical Co., both located within Iran). Double distilled water was used for preparing all solutions.

2.2. Preparation of PANI-PA-DBSA

Different amounts of DBSA (according to table 1) were added to 50 ml of chloroform and stirred for 5 minutes. At this point, a specified volume of freshly distilled aniline (with respect to stoichiometry of chemical oxidation reaction) was added to the solution under vigorous stirring leading to a homogeneous cloudy solution indicating micelle formation. After 10 minutes of stirring, chemical oxidation of aniline was initiated by drop-wise addition of a solution containing APS (An/APS=4/5) and 1 M PA dissolved in 50 ml of double distilled water, for 30 minutes. Stirring was continued for 1 hour at room temperature until a dark green solution (conductive form of PANI) was obtained. In order to break the emulsion and separate PANI-PA-DBSA, 20 ml of methanol (with respect to phase diagram of chloroform-methanol-water mixture) was added to the final solution. At this step, PANI-PA-DBSA remained in organic phase (Fig. 1) as a result of doping with DBSA. Organic phase of this biphasic solution was separated, using separatory funnel, and evaporated in a rotary evaporator. Resultant green paste was then washed thoroughly with 250 ml of ethanol/water (2:5 v/v) solution in order to remove aniline monomers, oligomers, and unreacted substrates. Finally, PANI-PA-DBSA powder was dried in an oven at 50 $^{\circ}$C overnight.

Table 1. Different amounts of substrate for chemical polymerization reaction (An/APS: 4/5)

Sample name	DBSA (gr)	PA (M)
DBSA 0	0	1
DBSA 0.2	0.2	1
DBSA 0.5	0.5	1
DBSA 1	1	1
DBSA 1.5	1.5	1
DBSA 2	2	1
DBSA 3	3	1

2.3. Formation of PANI-PA-DBSA epoxy paint

Different amounts of PANI-PA-DBSA were dissolved in desirable amount of xylene under stirring for 60 minutes. The solution was then filtered, to remove undispersed agglomerates, and added to a mixture containing Bisphenol-A-based epoxy resin and amine-based hardener (mixed according to manufacturer recommendations). Resultant mixture was homogenized for another 20 minutes to form final paint. Epoxy paint was dip-coated on carbon steel electrodes and allowed to cure in ambient temperature for one week.

2.4. Electrochemical setup

All electrochemical analyses were carried out using a Metrohm Autolab PGSTAT30 licensed for NOVA 1.10.4 software. A three-electrode setup was prepared for all electrochemical procedures. This setup consisted of an Ag/AgCl (filled with 3 M KCl solution) reference electrode, a platinum disk counter electrode (with surface area of 2 cm^2) and a carbon steel working electrode (with surface area of 1 cm^2). All working electrodes were made of API 5L X-52 brand new oil pipes. These electrodes were then polished using different sizes (220, 400, 600, 800, 1200, and 2000, respectively) of emery paper and ultrasonically degreased in a solution containing acetone and methanol. A double-jacketed cell and a water circulation system were used during electrochemical experiments to maintain steady temperature.
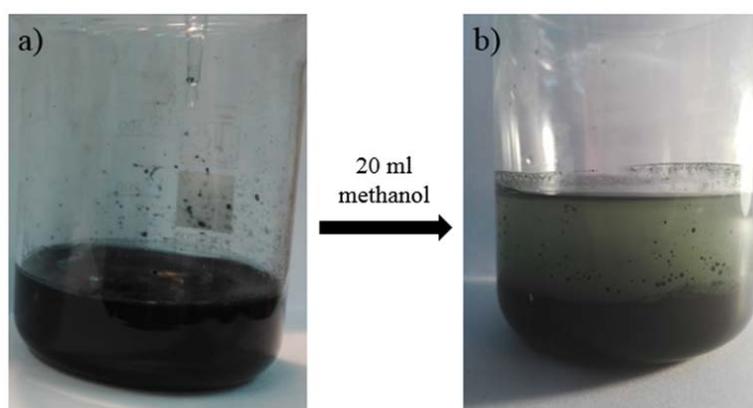

Fig. 1. Breaking chloroform-water emulsion; Monophasic solution (a) and biphasic solution after methanol addition (b)

3. RESULTS AND DISCUSSION

3.1. Polymerization of aniline

PANI is generally achieved via chemical oxidation in an acidic medium [40]. A wide range of oxidants are used in chemical oxidation of PANI. As a general rule, compounds with

high oxidation potentials (exceeding +1.0 V) are used to form conductive PANI. This is due to the fact that, chain formation reaction in acidic mediums has a relatively high energy barrier (+1.05 V). Hence, strong oxidizing agents such as persulfate and dichromate are preferred. However, weak oxidants of potentials lower than +1.0 V can also yield PANI, but not necessarily conductive PANI [41].Acidity of reaction medium is another key factor in polymerization of aniline. PANI preparation is possible within a very wide range of pH values (1-14). However, not all of the oxidation products, especially in weak acidic or basic conditions, can provide suitable conductivity or processability [42]. The importance of anionic dopants in polymerization of aniline is very well known, with their impact on conductivity, stability and solubility of PANI been widely investigated [43]. In this work, we have our focus on the optimization of both processability and corrosion protection performance of PANI using PA and DBSA as dopants. During bulk polymerization of aniline, undesirable branching and ortho-coupling reactions may result in non-dispersible PANI [44]. In order to prevent this phenomenon, the polymerization of aniline was proceeding in a heterogeneous medium containing chloroform and water. In this heterogeneous reaction, DBSA, which acts as both surfactant and dopant, will results in organic-dispersible PANI by favoring para-coupling of monomers and preventing unnecessary branching reactions [45]. As mentioned before, PA acts as an anticorrosion dopant by forming phosphate complexes on steel surface.

Polymerization of PANI-PA-DBSA proceeds through formation of anilinium–DBSA complex-like structures (Scheme. 2). Formed in organic phase, these structures have Krafft points similar to ionic surfactants [46], so that they may act as surfactants and form micelles at critical micelle concentration (CMC) [47]. At this point, it became obvious that, the formation of a milky solution before adding oxidant/acid solution is due to the formation of anilinium-DBSA reverse micelles.
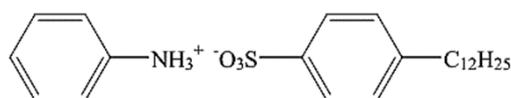
Scheme 2. Anilinium-DBSA complex

As it is illustrated in Fig. 2, when the aqueous phase containing APS and PA is added to previous solution, water and water soluble substrates trap inside reverse micelles. Polymerization of aniline is initiated through the formation of anilinium cation formed during the attack by initiators. This cation is polymerized to form PANI; at this stage, DBSA acts as an acidic dopant [48]. During the polymerization, the milky white solution will turn into a dark green solution, indicating the formation of conductive PANI emeraldine salt. Final

product of polymerization is PANI-PA-DBSA with some sulfate anionic dopants due to the presence of APS.

3.2. Polymerization conditions

3.2.1. Reaction time and temperature

Polymerization of aniline is an exothermic reaction which proceeds in three stages. Induction period is the first stage of the polymerization where anilinium cations and aniline oligomers are formed. During the next stage called polymerization period, these oligomers chain together via the formation of active species during polymer elongation process. During the polymerization period, temperature of reaction medium will steadily rise as the reaction goes on. At post polymerization stage when monomer, oxidant or both are already consumed, the polymerization reaction is considered as finished with the reaction mixture cooled down [25,49]. In order to increase polymerization yield and conductivity of PANI, the reaction is usually accomplished inside an ice bath at 5 ^{o}C. However, from industrial point of view, any heating or cooling step is seen as being energy consuming and hence increasing production expenses. As such, in the present work, polymerization reactions were carried out at room temperature. According to literature [50], polymerization of aniline at room temperature requires at least 10 minutes to complete. Therefore, polymerization reactions were continued for one hour to let the polymerization period settled down completely.
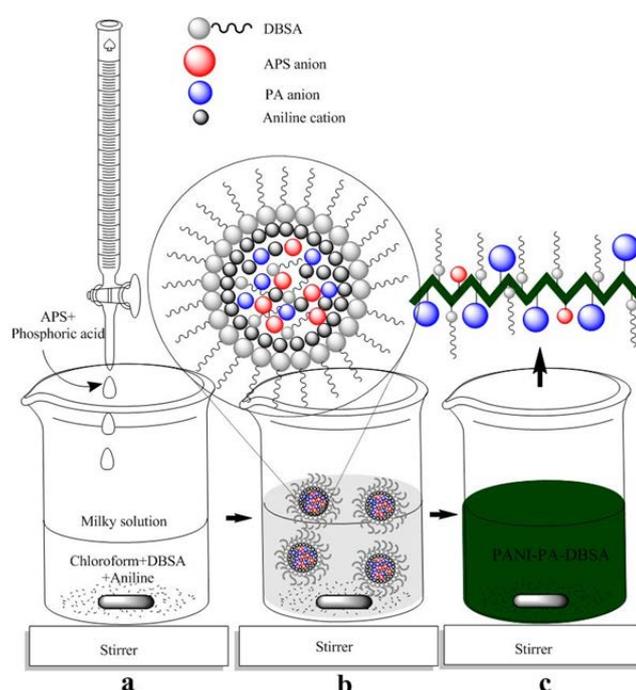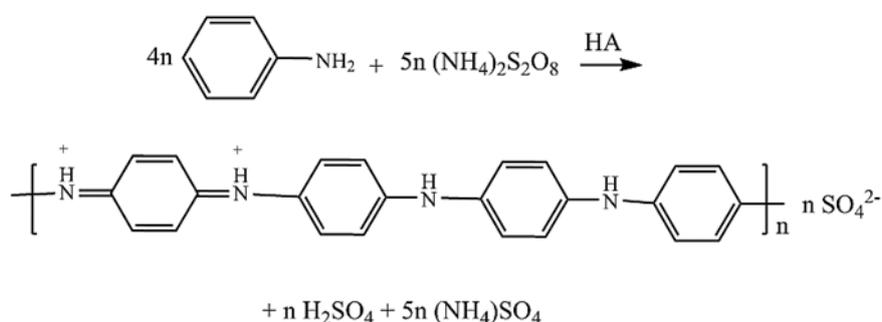

Fig. 2. PANI-PA-DBSA formation steps via chemical oxidation in three steps: formation of anilinium-DBSA complex (a); polymerization of aniline inside reverse micelles (b); and final product of polymerization (c)

3.2.2. Substrates concentration

According to stoichiometry of polymerization reaction (scheme. 3) monomer/oxidant ratio for chemical oxidation with APS was set to 4/5. Stejskal and Blinova reported that, chemical oxidation of PANI using 1 M solution of phosphoric acid yields a PANI of high conductivity. At high concentrations of phosphoric acid, phosphate anions are dominant counter ion in comparison to sulfate anions [25]. It was also reported that, thermal stability of the conductive PANI with its conduction coming from phosphate counter ions is higher than that of PANI doped with chloride anions [26]. Through choosing phosphate counter ions over other possible options, we tried to achieve PANI with relatively high stability and conductivity with potentially high performance as an anticorrosion material.

$$4n\ \langle\text{phenyl}\rangle\text{—NH}_2\ +\ 5n\ (NH_4)_2S_2O_8\ \xrightarrow{\ HA\ }$$

$$\left[\text{—N}^+\text{=}\langle\rangle\text{=N}^+\text{—}\langle\rangle\text{—}\underset{H}{N}\text{—}\langle\rangle\text{—}\underset{H}{N}\text{—}\langle\rangle\text{—} \right]_n \ n\ SO_4^{2-}$$

$$+\ n\ H_2SO_4\ +\ 5n\ (NH_4)SO_4$$

Scheme 3. The oxidation reaction of aniline with APS in acidic aqueous medium

3.3. Influence of DBSA

A series of experiments was carried out with different amounts of DBSA (Table 1). Samples containing high DBSA content showed paste-like glossy structures. With increasing DBSA concentration in the reaction medium, conductivity of final product was seen to decrease. That is probably due to binary role of DBSA. DBSA acts as both dopant and plasticizer, affecting intermolecular and intramolecular behaviors of PANI. At high concentration, DBSA penetrates into the intermolecular space and decreases PANI conductivity through increasing internal molecular motions which reduces crystallinity of PANI [51]. It was also noted that, when PANI with high DBSA content was used in paint formulation, final coating was ruptured. This phenomenon was directly related to DBSA content of PANI. As the internal motion of PANI molecules is increased, surface tension is also increased between polymer chains, creating some ruptures. These raptures reduce anticorrosion performance of the coating and should be avoided at any cost. Effect of DBSA content on rupture formation was investigated on glass samples (Fig. 3). In this experiment, three different PANI samples were used (DBSA 0, DBSA 1 and DBSA 3). When no DBSA is used during polymerization (DBSA 0), PANI is almost insoluble in xylene (paint solvent), so that the final coating becomes heterogeneous with rough surface which is far from ideal

conditions. As DBSA content is increased (DBSA 1), PANI becomes soluble in xylene and a homogeneous coating with smooth surface was formed. In excess of DBSA (DBSA 3), surface tension is increased, resulting in a ruptured yet smooth coating.

Fig. 3. Coatings containing PANI with different DBSA content. DBSA 0 (a); DBSA 1 (b) and DBSA 3 (c)

3.4. Characterization of PANI-PA-DBSA

Fig. 4 demonstrates the UV-Vis spectrum of PANI-PA-DBSA (DBSA 1) dissolved in chloroform. The three major peaks at around 340 nm (π-π^* transition of benzenoid rings), 430 nm (polaron-π^* transition in quinoid rings structures) and 710 (π-polaron transition of quinoid rings) indicate the conductivity of the synthesized PANI-PA-DBSA structures [52].
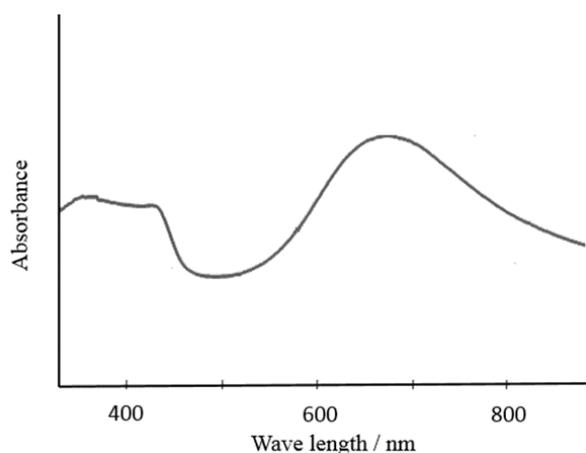

Fig. 4. UV-Vis spectrum of PANI-PA-DBSA (DBSA1) dissolved in chloroform

X-ray diffraction (XRD) pattern of PANI samples achieved by PHILIPS D6792 instrument is illustrated on Fig. 5. If only DBSA is used as the doping agent (PA 0), one may end up obtaining highly crystalline structures without amorphous phase with the corresponding XRD pattern been well-ordered. This is probably due to the formation of aniline oligomers or incomplete branches of PANI chains doped with DBSA in various locations. XRD patterns of all samples contain principal peaks of the PANI structure. The

peaks at 14.5∘, 19.8∘, and 25.2∘on Fig. 5 (a), (b) and (c) correspond to the (0 1 0), (0 0 1), and (1 1 0) reflections of PANI, respectively [39].
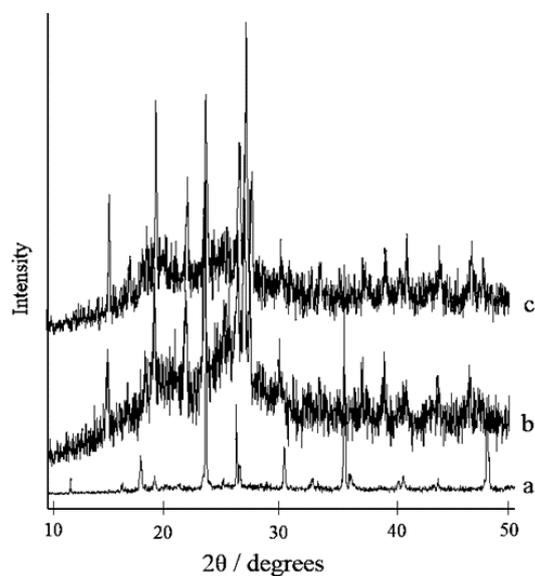

Fig. 5. XRD pattern of different PANI samples: PA 0 (a); DBSA 0 (b) and DBSA 1 (c)

FT-IR spectra of PANI base, DBSA and PANI-PA-DBSA are presented in Fig. 6. The characteristic peaks of these samples are reported in Table 2 [39 and 53].
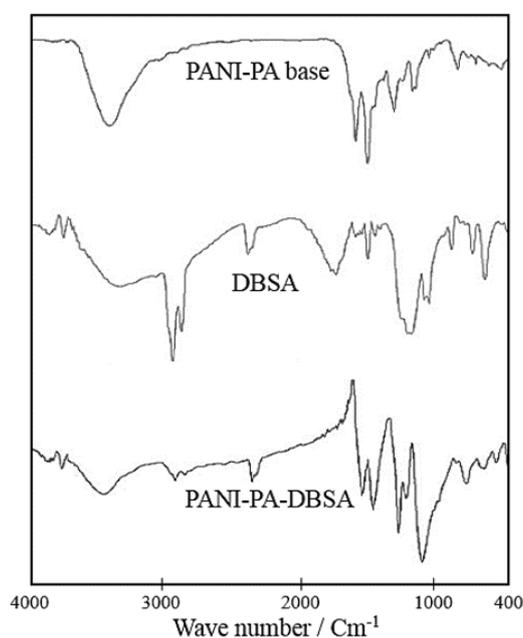

Fig. 6. FT-IR spectra of PANI-PA base, DBSA and PANI-PA-DBSA

The peak at 2θ=19.8∘ may be attributed to the shifts parallel to the polymer chain, and the peak at around 2θ=25.2∘ may be caused due to the alternation perpendicular to the polymer chain. This peak may also represent the characteristic distance between the ring planes of benzene rings in adjacent chains [53].

Table 2. Attribution of FT-IR spectra of different PANI samples

Attribution	PANI-PA base (Cm^{-1})	DBSA (Cm^{-1})	PANI-PA-DBSA (Cm^{-1})
N=Q=N	1128	1167	1126
C-N	-	1306	1297
C=C (Benzenoid)	1496	1504	1489
C=C (Quinoid)	-	1590	1559
C-H	832	832	801
O-H	3396	3428	3444
C-H (-CH$_2$)	2926	-	2922

3.5. Anticorrosion behavior of PANI-PA-DBSA

According to our previous work [54], the mechanism of protection of steel by PANI is schematically shown in Fig. 7. In neutral media, due to conductive capability of the coating, oxygen reduction reaction takes place on the polyaniline coating, while the oxidation of iron to its oxides takes place on the exposed iron surface at pinhole areas and under the film. In acidic conditions, the protection of pinholes is due to the cathodic reaction PANI (ES) ↔ PANI (LS). It is also proposed that, the polymer shifts the corrosion potential (E_{corr}) of the metal towards the passive region.
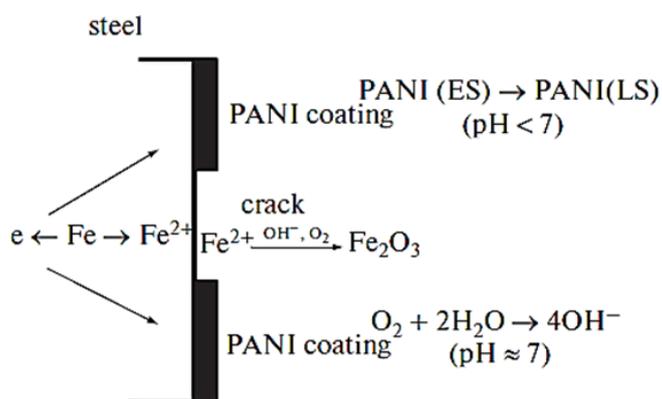

Fig. 7. Schematic diagram of iron passivation by PANI in neutral and acidic conditions

There is also evidence for a change in the cathodic reaction location, which is deemed to be due to the conductive nature of the coating. Thus, the reduction of oxygen to hydroxide shifts from the metal surface to the polymer/electrolyte interface and probably involves the reoxidation of the polymer [54].

Anticorrosion behavior of PANI-PA-DBSA coatings was carefully investigated using electrochemical techniques in 3.5% NaCl solution.

3.5.1. DC polarization plots

DC polarization curves for bare, epoxy-coated and PANI-PA-DBSA paints-coated carbon steel in NaCl 3.5% solution at 25 $^{\circ}$C are presented in Fig. 8.
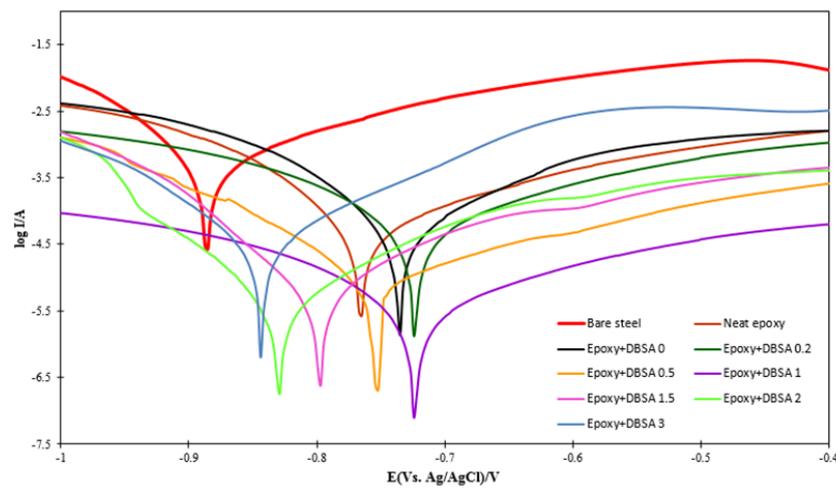

Fig. 8. DC polarization plots of various samples coated on carbon steel in 3.5% NaCl solution

Table 3. Parameters of DC polarization curves for bare and coated carbon steel in 3.5% NaCl solution

Sample name	I_{Corr} (µA)	E_{Corr} (mV)
Bare steel	95.5	-880.1
Neat epoxy	13.2	-770.6
Epoxy+DBSA 0	11.2	-733.1
Epoxy+DBSA 0.2	10.0	-721.0
Epoxy+DBSA 0.5	3.1	-750.0
Epoxy+DBSA 1	0.6	-725.3
Epoxy+DBSA 1.5	1.4	-796.2
Epoxy+DBSA 2	1.2	-830.5
Epoxy+DBSA 3	6.3	-840.0

The associated electrochemical parameters were calculated from the polarization plots and are reported in Table 3. It can be observed that, corrosion current of the coating containing DBSA 1 is decreased while its corrosion potential is moved toward more positive region. This is probably due to the increase in PANI-PA-DBSA processability which is caused by DBSA-doped PANI chains. Corrosion current density of DBSA 1.5, DBSA 2 and DBSA 3 samples were observed to increase with DBSA content. This could be due to the formation of cracks within coatings, caused by high surface tension, when using high concentrations of surfactant during polymerization.

3.5.2. EIS measurements of coated samples

EIS data on corrosion protection of PANI-PA-DBSA is presented in the form of nyquist plots. The Nyquist plot format makes it easy to evaluate effects of ohmic resistance.
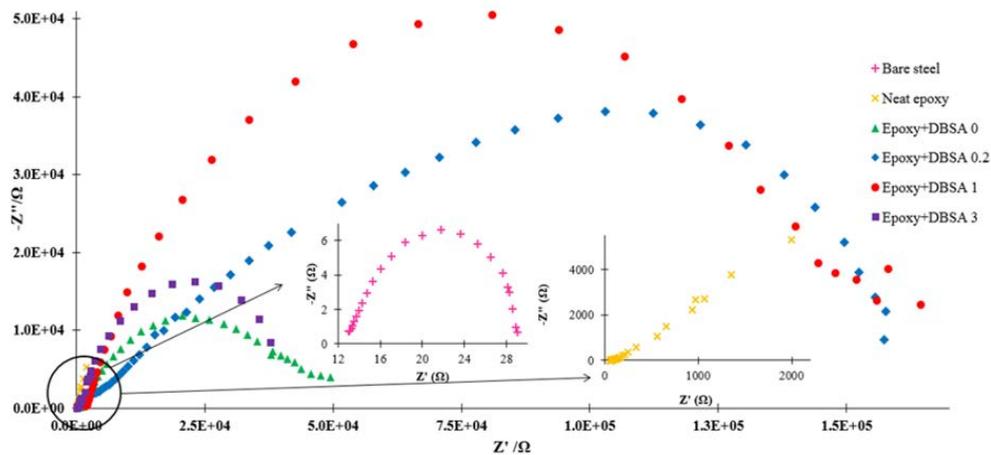

Fig. 9. Nyquist plots of different coated samples in 3.5% NaCl solution
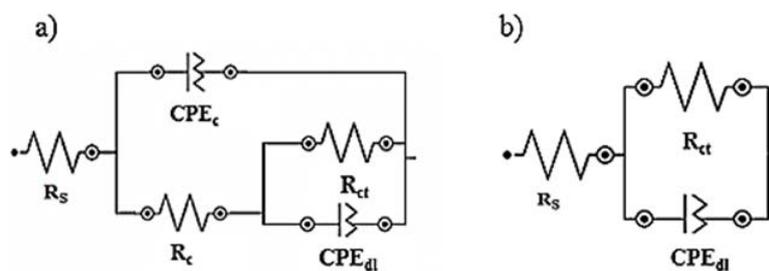

Fig. 10. ECM used for modeling impedance data in 3.5% NaCl solution for coated (a) and bare steel (b) samples

With these plots, it is also relatively easy to compare different samples according to semicircle shapes and position at different frequencies. EIS measurements were carried out using a three-electrode system at OCP potential at frequencies ranging from 0.01 (Hz) up to

10^5 (Hz). Impedance data was processed using Z View 3.3 and fitted to proper electrical equivalent circuit (ECM) to calculate EIS parameters.

Nyquist plots of different carbon steel samples are presented in Fig. 9. The ECM used for modeling these samples is demonstrated on Fig. 10. The plots are composed of a semi-circle at high frequencies, which is related to Faradaic reactions. The linear curve in low frequency region can be attributed to the diffusion-controlled process in the electrolyte. The initial non-zero intercept at Z' at the beginning of the semi-circle is almost identical along all curves; it is due to the electrical resistance of electrolyte. The resistance projected by the semi-circle is due to that of the active electrode material [56]. The ECM consists of resistance (R) and constant phase elements (CPE). The impedance of CPE can be expressed as $Z_{CPE} = 1/_{Y_0(j\omega)^n}$ where Y_0 is the admittance of an ideal capacitance, ω is angular frequency and equal to $2\pi f$ where f denotes linear frequency, j is equal to $\sqrt{-1}$, and n is an empirical constant ranging from 0 to 1. For $n=1$, the impedance of CPE is pure capacitance. The true capacitance can be estimated from CPE using the relationship $C = R^{(\frac{1-n}{n})}CPE^{(\frac{1}{n})}$. The ECM parameter R_S, R_c and R_{ct} are electrolyte solution resistance, the resistance of the coating and charge transfer resistance, respectively, with CPE_{dl} formed at electrical double layer and CPE_c formed at the coating [57]. Estimated impedance parameters of the samples in Fig. 9 are presented in Table 4.

Table 4. Impedance parameters of different coating in 3.5% NaCl

Sample name	R(Ω cm^2)	C (F cm^{-2})
Bare electrode	20.82 (R$_{ct}$)	2.26×10^{-9} (C$_{dl}$)
Neat epoxy	2.53×10^4 (R$_c$)	2.26×10^{-7} (C$_c$)
Epoxy+DBSA 0	4.65×10^4(R$_c$)	2.68×10^{-7}(C$_c$)
Epoxy+DBSA 0.2	1.36×10^5(R$_c$)	1.51×10^{-7}(C$_c$)
Epoxy+DBSA 1	1.78×10^5(R$_c$)	8.66×10^{-7}(C$_c$)
Epoxy+DBSA 3	3.11×10^4(R$_c$)	3.19×10^{-7}(C$_c$)

According to Table 5, the highest resistance and capacitance were achieved for the coating containing DBSA 1, $1.8×10^5$ and $8.66×10^{-5}$ respectively.

3.5.3. Open circuit potential measurements

Open circuit potential (OCP) of various coatings *vs.* Ag/AgCl in 3.5% NaCl solution are shown in Fig. 11. Three time periods can be recognized obvious during OCP evaluation: 1) a sharp decrease in OCP at the beginning which corresponds to solvent diffusion in coating, 2) an increase in OCP with time, which is attributed to the formation of passive oxide layer, and 3) OCP stability. The increase in OCP of the coated samples during immersion indicates that,

coated specimens are in passive states and the metal is protected [55]. The OCP value of the PANI-PA-DBSA coating containing 1 gr of DBSA (DBSA 1) stabilized faster and remained more stable throughout time.
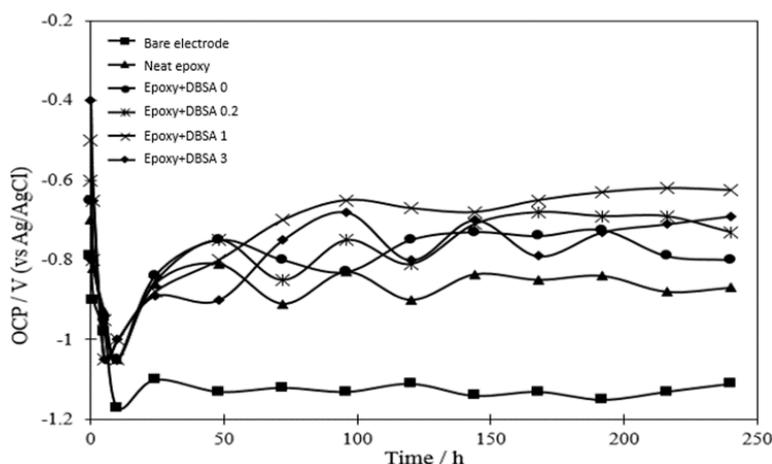

Fig. 11. OCP-time curves of various coatings coated on carbon steel in 3.5% NaCl solution

3.6. Morphology of coating

SEM images of various PANI samples are presented on Fig. 12. As it was proposed before, the formation of PANI oligomers instead of PANI polymers results in crystalline-like structure. These needle-like structures are observed in Fig. 14 a. In the case of DBSA 1 (Fig. 12 c), a fine and nearly uniform structure is observed as a result of emulsion polymerization, while when no DBSA is added, bulky structures are achieved due to bulk polymerization.
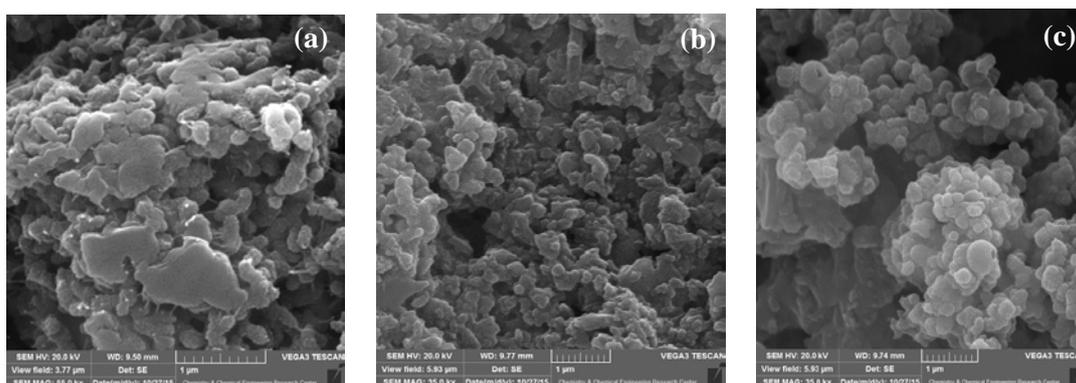

Fig. 12. SEM images of PA 0 (a); DBSA 0 (b) and DBSA 1 (c) Sample

4. CONCLUSION

In this work, soluble PANI-PA-DBSA, as a suitable additive for paint formulations, was successfully prepared. PANI-PA-DBSA was then added to epoxy resin and dip coated on carbon steel specimens. Conductive nature of this polymer was investigated using different

techniques. Corrosion protection efficiency of different samples with various surfactant contents was investigated using electrochemical techniques. According to DC polarization plots, the addition of DBSA could move corrosion potential of carbon steel toward more positive potentials and effectively decrease corrosion current. Further, impedance studies of different coatings indicated that, coating resistance and capacitance were affected by DBSA content. It was noted that, when DBSA content was too high, corrosion protection efficiency decreased due to the formation of cracks within the coating. According to the results, the PANI-PA-DBSA containing 1 gr of DBSA exhibited stronger anticorrosion characteristic. OCP of this sample stabilized faster and showed little fluctuation throughout investigation time. It was also shown that, the sample containing 1g of DBSA exhibit more uniform structure due to the emulsion polymerization reaction. The XRD pattern of this sample showed so-called conductive PANI structure. In general, PANI-PA-DBSA (DBSA 1) showed better anticorrosion characteristics compared to other samples.

REFERENCES

[1]   S. P. Sitaram, J. O. Stoffer, and T. J. O'Keefe, J. Coat. Technol. 69 (1997) 65.

[2]   W. Deberry, J. Electrochem. Soc. 132 (1985) 102.

[3]   E. Akbarinezhad, M. Ebrahimi, and H. R. Faridi, Prog. Org. Coat. 64 (2009) 361.

[4]   J. L. Camalet, J. C. Lacroix, S. Aeiyach, K. Chane-Ching, and P. C. Lacaze, Synth. Met. 93 (1998) 133.

[5]   A. G. MacDiarmid, Synth. Met. 84 (1997) 27.

[6]   Y. Bin, W. Gengchao, J. Ye, and X. Li, Mater. Lett. 62 (2008) 1775.

[7]   R. Gasparac, and C. R. Martin, J. Electrochem. Soc. 149 (2002) B409.

[8]   S. de Souza, J. E. P. da Silva, S. I. C. de Torresi, M. L. A. Temperini, and R. M. Torresi, Electrochem. Solid-State Lett. 4 (2001) B27.

[9]   X. Yang, B. Li, H. Wang, and B. Hou, Prog. Org. Coat. 69 (2010) 267.

[10] S. Sathiyanarayanan, S. Muthukrishnan, G. Venkatachari, and D. C. Trivedi, Prog. Org. Coat. 53 (2005) 297.

[11] J. L. Forveille, and L. Olmedo, Synth. Met. 65 (1994) 5.

[12] Y. Wang, X. Jing, and J. Kong, Synth. Met. 157 (2007) 269.

[13] J. Stejskal, M. Trchova, J. Kovarˇova, L. Brozˇova, and J. Prokeš, React. Funct. Polym. 69 (2009) 86.

[14] R. Ullah, G. A. Bowmaker, C. Laslau, G. I. N. Waterhouse, Z. D. Zujovic, K. Ali , A. Ali Shah, and J. Travas-Sejdic, Synth. Met. 198 (2014) 203.

[15] G. M. Morales, M. C. Miras, and C. Barbcro, Synth. Met. 101 (1999) 686.

[16] J. Stejskal, D. Hlavata, P. Holler, M. Trchova´, J. Prokesˇ, and I. Sapurina, Polym. Int. 53 (2004) 294.

[17] A. Pud, N. Ogurtsov, A. Korzhenko, and G. Shapoval, Prog. Polym. Sci. 28 (2003) 1701.

[18] A. Raki´, S. Trifunovi´, and G.´Ciri´c-Marjanovi´, Synth. Met. 192 (2014) 56.

[19] W. Li, and M. Wan, J. Appl. Polym. Sci. 4 (1999) 615.

[20] C. Jeyaprabha, S. Sathiyanarayanan, and G. Venkatachiari, J. Electroanal. Chem. 583 (2005) 232.

[21] T. P. McAndrew, Trends Polym. Sci. 5 (1997) 7.

[22] P. J. Kinlen, V. Menon, and Y. Ding, J. Electrochem. Soc. 146 (1999) 3690.

[23] S. Sathiyanarayanan, S. Muthkrishnan, and G. Venkatachari, Electrochim. Acta 51 (2006) 6313.

[24] I. Šeděnková, M. Trchová, N. V. Blinova, and J. Stejskal, Thin Solid Films 515 (2006) 1640.

[25] N. V. Blinova, J. Stejskal, M. Trchova´, and J. Prokes, Polymer 47 (2006) 42.

[26] P. J. Stejskal, J. Polym Degrad Stab 86 (2004) 187.

[27] J. E. P. da Silva, S. I. C. de Torresi, and R. M. Torresi, Corr. Sci. 47 (2005) 811.

[28] S. Sathiyanarayanan, S. Syed Azim, and G. Venkatachari, Synth. Met. 157 (2007) 205.

[29] S. Bilal, S. Gul, R. Holze, and A. Ali Shah, Synth. Met. 206 (2015) 131.

[30] N. Bahrami Panah , M. Payehghadr, I. Danaee, H. Nourkojouri, and M. Sharbatdaran, Iran Polym. J. 21 (2012) 747.

[31] F. Xavier Perrin, T. Anh Phan, and D. Lam Nguyen, Eur. Polym. J.66 (2015) 253.

[32] O. sterholm JE, C. Y, F. Klavetter, and P. Smith, Synth. Meter. 55 (1993) 1034.

[33] S. Palaniappan, and A. John, Prog. Polym. Sci. 33 (2008) 732.

[34] X. M. Sui, Y. Chu, S. X. Xing, and C. Z. Liu, Mater. Lett. 58 (2004) 1255.

[35] X. M. Sui, Y. Chu, S. X. Xing, Y. Min, and C. Z. Liu, Colloids Surf. A 251 (2004) 103.

[36] E. M. Egorova, and A. A. Revina, Colloids Surf. A 168 (2000) 87.

[37] D. X. Liu, J. L. Zhang, B. X. Han, J. Chen, Z. H. Li, D. Shen, and G. Y. Yang, Colloids Surf. A 227 (2003) 45.

[38] W. D. Sun, L. P. Xu, Y. Chu, and W. Shi, J. Colloid Interf. Sci. 266 (2003) 99.

[39] Y. Hana, T. Kusunose, and T. Sekino, Synth. Met. 159 (2009) 123.

[40] A. G. MacDiarmid, J. C. Chiang, A. F. Richter, N. L. D. Somasiri, A. J. Epstein, and L. Alcacer, Reidel Dordrecht (1987) 105.

[41] S. Yu, J. Stejskal, Russian J. General Chem. 82 (2012) N2 256.

[42] J. Stejskal, I. Sapurina, and M. Trchová, Prog. Polym. Sci. 35 (2010) 1420.

[43] J. Stejskal, Pure Appl. Chem.74 (2002) 857.

[44] E. Genies, C. J. Tsintavis, Electroanal. Chem. 195 (1985) 109.

[45] S. Lee, D. H. Lee, K. Lee, and C. W. Lee, Adv. Funct. Mater. 15 (2005) 1495.

[46] Y. Hana, T. Kusunose, and T. Sekino, Synth. Met. 159 (2009) 123.

[47] Y. Han, S. G. Oh, S. I. Shin, W. D. Joung, S. C. Yi, and C. G. Cho, Colloids Surf. B 24 (2002) 33.

[48] M. Oh, S. Kim, Electrochim. Acta 59 (2012) 196.

[49] I. Sapurina, and J. Stejskal, Polym. Int. 57 (2002) 1295.

[50] H. Yoon, B. Jung, and H. Lee, Synth. Met. (41) 1991699.

[51] A. G. MacDiarmid, and A. J. Epstein, Synth. Met. 65 (1994) 103.

[52] R. Arefinia, A. Shojaei, H. Shariatpanahi, and J. Neshati, Prog. Org. Coat. 75 (2012) 502.

[53] J. P. Pouget, M. E. Jozefowicz, A. J. Epstein, X. Tang, and A. G. MacDiarmid, Macromolecules 24 (1991) 779.

[54] P. Ghosh, S. K. Siddhanta, and A. Chakrabarti, Eur. Polym. J. 35 (1999) 699.

[55] M. Khanmohammadi, F. Mizani, M. Barzegar Khaleghi, and A. Bagheri Garmarudi, Prot. Met. Phys. Chem. 49 (2013) 661.

[56] H. Li, X. Wang, J. Li, and F. Wang, Corros. Sci. 53 (2011) 4044.

[57] C. Tan, and D. J. Blackwood, Corros. Sci. 45 (2003) 545.

[58] M. White, E. D. Wachsman, and V. Thangadurai, J. Mater. Chem. A, 2 (2014) 2363.